Solar Powered Closed-loop Current Controlled DC-DC Buck Converter for Battery Charging Application

Chetan S. Matwankar
Dept. of Electrical and Electronics Engineering
Birla Institute of Technology
Mesra, India
chetanmatwankar@gmail.com

Aftab Alam
Dept. of Electrical and Electronics Engineering
Birla Institute of Technology
Mesra, India
aftabalam5555@gmail.com

***Abstract*— Due to the intermittent nature of renewable energy sources (RESs), there exists a need for a storage system like a battery. The work presented in this paper consists of a solar photovoltaic powered battery charger using a current controlled dc-dc buck converter for charging a high capacity battery bank. The mathematical modeling of the converter using a state space approach is also presented.**

***Keywords*— battery charger, buck converter, solar photovoltaic, state-space**

I. Introduction

There is a global drive of moving towards cleaner and greener energy due to the concerns of climate change and the fast depletion of fossil fuels [1]. This has led to a renewed focus for developing technologies to harness the energy available from the renewable energy sources for electric power generation. The most popular renewable energy source is solar energy due to its availability for a longer period of time as compared to other sources. However, all renewable energy sources including solar energy are required to be used with an energy storage system such as a battery. The stored energy can be utilized to power the load during unavailability of the RES.

Rechargeable batteries are very common in renewable energy-based power generation systems for the storage of energy. Battery charging also plays a critical role in the design of electric vehicles [2][3]. A lot of research is being done in the field of battery management as evident from [4][5]. The most widely used type of batteries for energy storage used in isolated photovoltaic (PV) systems are lithium-ion (Li-ion) and batteries with lead-acid as electrolyte. The Li-ion batteries have many desirable properties such as good life cycle, high specific energy, high energy density and are environment-friendly. Hence these batteries have evolved as a popular choice for use in renewable energy-based systems [6][7][8].

This paper presents a method of utilizing the energy obtained from the solar PV modules to charge the Li-ion battery bank using a dc-dc buck converter which operates in constant current controlled topology. The duty ratio of the buck converter is controlled using a PI controller tuned by the Ziegler-Nichols method. A mathematical model of the buck converter is developed using a state-space modeling approach. A MATLAB based simulation is done for tuning the parameters of the controller. The results obtained are then verified experimentally.

II. Mathematical Modeling

The power circuit diagram of a dc-dc step down buck converter is shown in Fig. 1. The state-space model for the buck converter cannot be obtained directly as the circuit changes each time during the switching action. Hence the model is obtained using the circuit averaging technique. In this technique, the state-space models are obtained for each mode of operation and then to obtain the final steady-state model, the time averaging technique is applied.

A. During ON period of the switch

The equivalent circuit diagram of the buck converter is as shown in Fig. 2. During this period,

$$\frac{di_{LB}}{dt} = \frac{-1}{L} V_{CB} + \frac{1}{L} V_{in} \tag{1}$$

$$\frac{dV_{CB}}{dt} = \frac{1}{C} i_{LB} - \frac{1}{RC} V_{CB} \tag{2}$$

These equations can be represented using the state model of the form,

$$\dot{x} = A_1 x + B_1 u \tag{3}$$

$$y = C_1 x + D_1 u \tag{4}$$

where,

$$A_1 = \begin{bmatrix} 0 & \frac{-1}{L} \\ \frac{1}{C} & \frac{-1}{RC} \end{bmatrix}$$

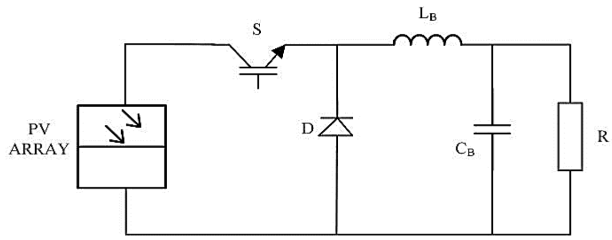

Fig. 1 Circuit Diagram of dc-dc Buck Converter

978-1-5386-9353-7/19/$31.00 ©2019 IEEE

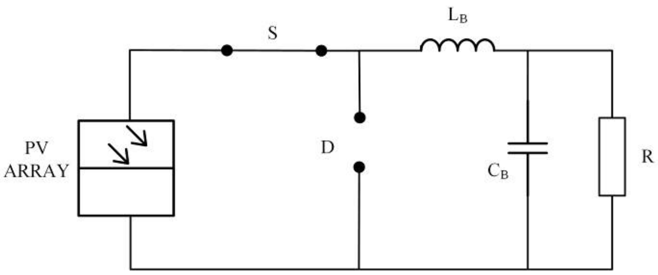

Fig. 2 Equivalent diagram of buck converter during ON period

$$B_1 = \begin{bmatrix} \frac{1}{L} \\ 0 \end{bmatrix}$$

$$C_1 = \begin{bmatrix} 0 & 1 \end{bmatrix}$$

$$D_1 = 0$$

B. During OFF period of the switch

The equivalent circuit of the buck converter is as shown in Fig. 3. During OFF period,

$$\frac{di_L}{dt} = \frac{-1}{L} V_C \tag{5}$$

$$\frac{dV_C}{dt} = \frac{1}{C} i_L - \frac{1}{RC} V_C \tag{6}$$

These equations can be represented using the state model of the form,

$$\dot{x} = A_2 x + B_2 u \tag{7}$$

$$y = C_2 x + D_2 u \tag{8}$$

where,

$$A_2 = \begin{bmatrix} 0 & \frac{-1}{L} \\ \frac{1}{C} & \frac{-1}{RC} \end{bmatrix}$$

$$B_2 = \begin{bmatrix} 0 \\ 0 \end{bmatrix}$$

$$C_2 = \begin{bmatrix} 0 & 1 \end{bmatrix}$$

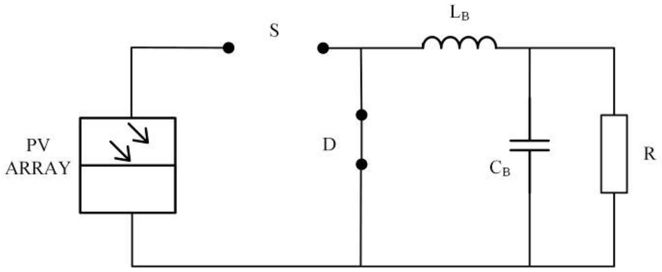

Fig. 3 Circuit diagram of dc-dc buck converter during OFF period

$$D_2 = 0$$

C. Obtaining the final state-space model using circuit averaging technique

Now, considering the duty cycle to be,

$$d = \frac{T_{ON}}{T_S} \tag{9}$$

$where\ T_s = T_{ON} + T_{OFF}$

The ON period will be dT_s and the OFF period will be (*1-d*)Ts. Hence, the model 1 will be applicable for dT_s period and model 2 will be applicable for $(1-d)T_s$ period.

By circuit averaging technique, the complete state-space matrices can be found as,

$$A = A_1 d + A_2(1-d)$$

$$B = B_1 d + B_2(1-d)$$

$$C = C_1 d + C_2(1-d)$$

$$D = D_1 d + D_2(1-d) \tag{10}$$

So, the final state-space matrices are obtained as,

$$A = \begin{bmatrix} 0 & \frac{-1}{L} \\ \frac{1}{C} & \frac{-1}{RC} \end{bmatrix}$$

$$B = \begin{bmatrix} \frac{d}{L} \\ 0 \end{bmatrix}$$

$$C = \begin{bmatrix} 0 & 1 \end{bmatrix}$$

$$D = 0 \tag{11}$$

The above state space model can be used to obtain the system transfer function for applying control techniques to obtain the desired response.

III. CLOSED LOOP CONTROL MODE OF THE BUCK CONVERTER

The buck converter can be made to operate in two modes for the battery charging application:

1. Constant Load Voltage Mode
2. Constant Load Current Mode

In this paper, the constant load current mode is implemented as it takes care of the variations in the battery terminal voltage during the charging process.

The block diagram for the closed-loop current control of the dc-dc step down buck converter is shown in Fig. 4.

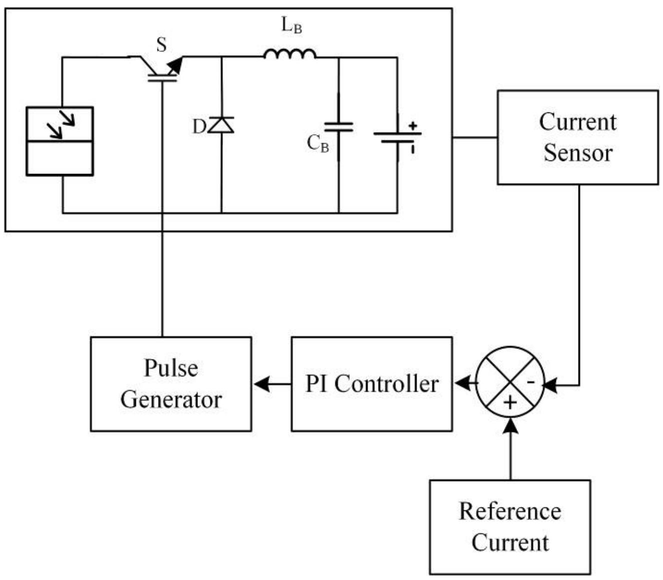

Fig. 4. Block diagram of closed-loop current control of buck converter

The output current is sensed, supplied back and compared with a reference value to produce an error signal. The error signal is then fed to a PI controller in order to keep the output current constant. The parameters of the PI controller are tuned using the Ziegler-Nichols tuning technique to obtain the desired response.

IV. MATLAB/SIMULINK BASED SIMULATION

The above system is simulated using SIMULINK in order to tune the parameters. The simulation model is shown in Fig.5.

The proper choice of the inductor and capacitor is important in order to have the ripples in the current and voltage respectively under acceptable limit.

The inductor can be selected based on the limit of current ripple as shown in [8].

$$L = \frac{V_{PV}d(1-d)}{\Delta If} \tag{12}$$

where, ΔI is the peak--peak ripple in the inductor current while *f* is the gate switching frequency.

Similarly, the capacitor is to be selected by considering the ripple voltage [8].

$$C = \frac{V_{PV}d(1-d)}{8Lf^2\Delta V_C} \tag{13}$$

where ΔV_C is the peak-peak ripple in the capacitor voltage.

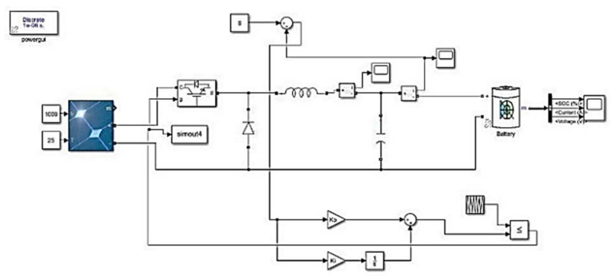
Fig. 5 Simulation Model of the scheme

Fig. 6 to Fig. 9 show the simulation model results.

The battery charging current is shown in Fig. 6. The negative value indicates the current direction is towards the battery, i.e. charging mode. Also, the state of charge (SOC) i.e. the charging status of the battery is steadily increasing.

V. HARDWARE IMPLEMENTATION

A. Design of Snubber circuit for the IGBT

At the instant of switch turn-off, the voltage across the IGBT shoots up to a very high value due to a large dv/dt surge appearing across the switch due to current interruption through the inductor. This high voltage surge may result in the switch getting damaged. To protect the switch, a turn-off RCD snubber is connected across the IGBT. The value of the snubber circuit components is decided as follows [9],

$$C = \frac{i_{LOAD}t_f}{2V_{PV}} \tag{14}$$

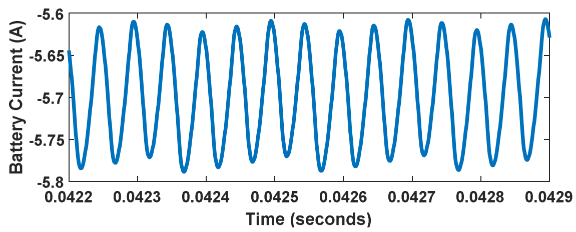

Fig. 6 Charging Current of the Battery

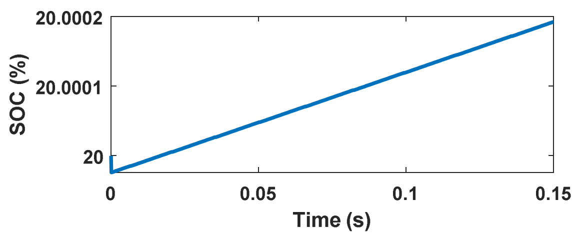

Fig. 7 State of charge (SOC) of the Battery

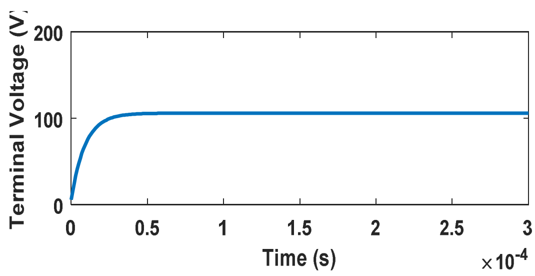

Fig. 8 Battery terminal voltage

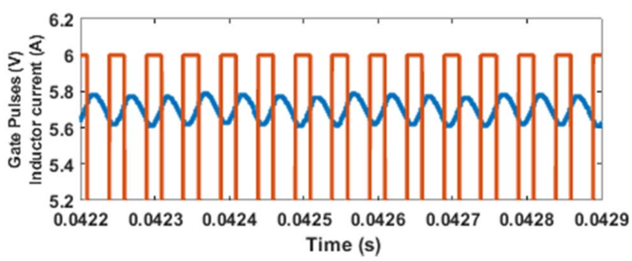

Fig. 9 Gate pulses to the switch and current through the inductor

$$\frac{V_{PV}}{I_{CEmax} - i_{LOAD}} < R < \frac{(T_{on})_{min}}{5C} \qquad (15)$$

where I_{CEmax} is the maximum permissible collector-emitter current through the switch and $(T_{on})_{min}$ is the minimum time period for which the switch remains ON in the circuit.

The circuit parameters are as given in table I and II.

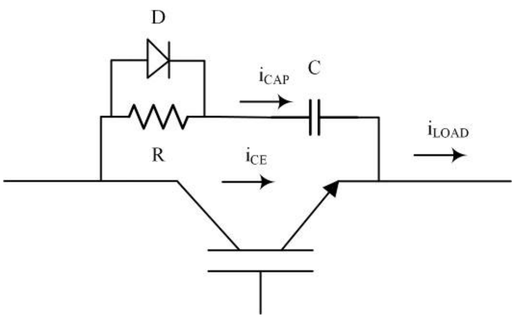

Fig. 10 Turn-OFF Snubber circuit

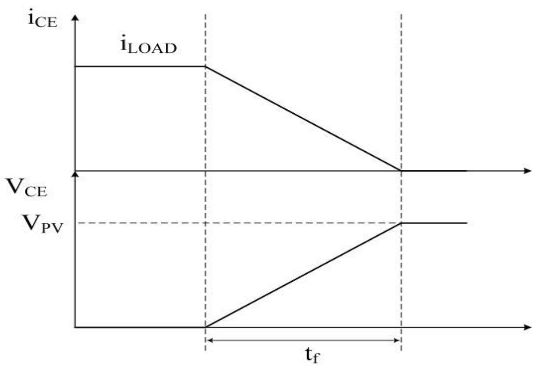

Fig. 11 Voltage and Current across the switch during turn-OFF

TABLE I
CIRCUIT PARAMETERS OF THE BUCK CONVERTER

Sr. No.	Parameter	Value
1	Capacitance CB	470 µF
2	Inductance L	10 mH
3	Snubber Capacitance	220 nF
4	Snubber Resistance	4.7 Ω
5	Battery Bank Rating	110AH, 100V

TABLE II
RATINGS OF THE SOLAR PV ARRAY

Sr. No.	Parameter	Value
1	Open Circuit Voltage	188.4 V
2	Short Circuit Current	33.33 A
3	Maximum Rated Voltage	154.8 V
4	Maximum Rated Current	32.44 A
5	Rated Power	5.021 kW

B. *Current Sensor Calibration*

Here, as the current is the controlled element, the correct sensing of the output current is critical for the proper operation of the PI controller. Hence an accurate current sensor along with its proper calibration is required.

In the present work, the current sensor used is LA100 of LEM make. For the calibration of the sensor, a known value of current was passed through the sensor and its output voltage was measured. These readings taken were plotted as shown in Fig. 12 and the equation of the curve were obtained. This equation was fed into the microcontroller to convert the input analog voltage to its equivalent current value.

C. *Experimental Results*

The waveform of the inductor current is shown in Fig.13.

VI. CONCLUSION

This paper presents a simple method of charging a high capacity battery bank using a buck converter in constant current control mode. The battery is being charged at a steady rate of flow of current of 6 A. The parameters of the controller are tuned using the Ziegler-Nichols tuning method. The mathematical model of the buck converter using a state-space approach is also presented.

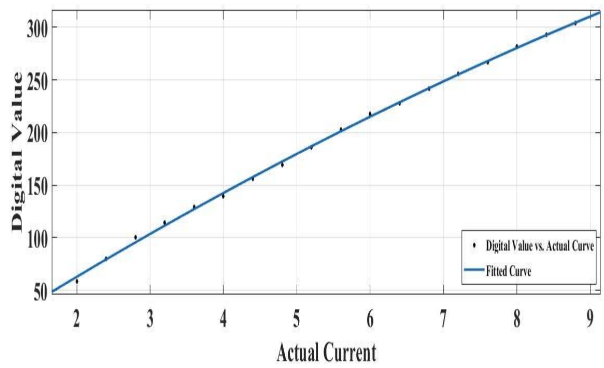

Fig. 12 Current Sensor calibration curve

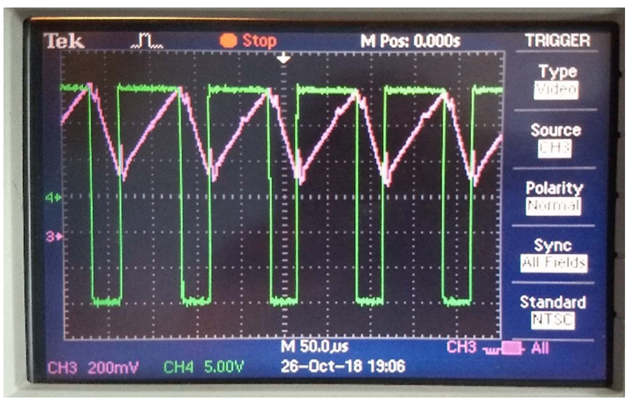

Fig. 13 Inductor current waveform from the experimental setup

VII. REFERENCES

[1] S. K. Soonee, V. K. Agrawal, P. K. Agarwal, S. R. Narasimhan and M. S. Thomas, "The View from the Wide Side: Wide-Area Monitoring Systems in India," *IEEE Power and Energy Magazine*, vol. 13, no. 5, pp. 49-59, Sept.-Oct. 2015

[2] K. R. Reddy and S. Meikandasivam, "Load Flattening and Voltage Regulation using Plug-In Electric Vehicle's Storage capacity with Vehicle Prioritization using ANFIS," *IEEE Transactions on Sustainable Energy* (in press).

[3] R. Xiong, J. Cao, Q. Yu, H. He and F. Sun, "Critical Review on the Battery State of Charge Estimation Methods for Electric Vehicles," *IEEE Access*, vol. 6, pp. 1832-1843, 2018.

[4] V. Karthikeyan and R. Gupta, "Multiple-Input Configuration of Isolated Bidirectional DC-DC Converter for Power Flow Control in Combinational Battery Storage," *IEEE Transactions on Industrial Informatics*, vol. 14, no. 1, pp. 2-11, Jan. 2018.

[5] C. Zou, C. Manzie and D. Nešić, "Model Predictive Control for Lithium-Ion Battery Optimal Charging," *IEEE/ASME Transactions on Mechatronics*, vol. 23, no. 2, pp. 947-957, April 2018

[6] N. Tashakor, E. Farjah and T. Ghanbari, "A Bidirectional Battery Charger With a Modular Integrated Charge Equalization Circuit," *IEEE Transactions on Power Electronics*, vol. 32, no. 3, pp. 2133-2145, March 2017.

[7] L. Patnaik, A. V. J. S. Praneeth and S. S. Williamson, "A Closed-Loop Constant-Temperature Constant-Voltage Charging Technique to Reduce Charge Time of Lithium-Ion Batteries," *IEEE Transactions on Industrial Electronics*, vol. 66, no. 2, pp. 1059-1067, Feb. 2019.

[8] M. H. Rashid, “Power Electronics: Devices, Circuits and Applications”, *Pearson*, 2018

[9] L. Umanand, “Power Electronics: Essentials and Applications”, *Wiley India*, 2016